

Electrospinning and characterization of alumina borosilicate ceramic nanofibres

S. TANRIVERDI¹, B. MAVIS^{2*}, G. GÜNDÜZ¹, Ü. ÇOLAK³

¹Kimya Mühendisliği Bölümü, Ortadoğu Teknik Üniversitesi, Ankara 06531, Turkey

²Makina Mühendisliği Bölümü, Hacettepe Üniversitesi, Beytepe Ankara 06800, Turkey

³Nükleer Enerji Mühendisliği Bölümü, Hacettepe Üniversitesi, Beytepe Ankara 06800, Turkey

Alumina borosilicate/polyvinylalcohol (PVA) composite nanofibres were prepared by the sol-gel method and electrospinning technique. Effects of solution viscosity, applied voltage, capillary tip to metal collector distance and calcination temperature were evaluated by scanning electron microscopy, X-ray diffraction, Fourier transform infrared spectroscopy and thermogravimetric/differential thermal analysis. Results indicate that while the initial fibre diameters can be fine-tuned with the right choice of alkoxide-solvent-polymer system and experimental set-up parameters (voltage and capillary tip to collector distance), the final fibre diameter, crystalline phase and morphology of alumina borosilicate fibres are largely influenced by the calcination temperature.

Key words: *electrospinning; sol-gel; nanofibre; alumina; boron; silicate*

1. Introduction

Alumina, silica and boron oxide based fibre present properties important in various applications including thermal protection, composite reinforcement and adsorption in diesel engine filters [1–6]. Alumina fibres, which have poor mechanical properties at high temperatures but good durability and mechanical properties in oxidizing environments, have been successfully prepared using melt cooling and sol-gel methods [1, 2]. On the other hand, aluminum borate fibres have attracted more attention due to their stability at high temperatures. Readey produced $Al_{18}B_4O_{33}$ whisker-like grains and found that aluminum borate phase was stable up to 1700 °C [6].

Recently the use of electrospinning technique for the production of ceramic nanofibres has been on the rise. More than 20 oxide and mixed oxide systems including

*Corresponding author, e-mail: bmavis@hacettepe.edu.tr

silicates and aluminium-borate have been electrospun successfully [7–17]. Silica based nanofibres which have unique properties like high thermal resistance with self-extinguishing character and promise for space-based applications or applications like optoelectronic devices, were synthesized via slight variations in the electrospinning technique [13–16]. Dai et al. have electrospun aluminum-borate oxide system into ultra-fine nanofibres which could potentially be used in ceramic filters and ceramic–metal composites [17].

In this work, applicability of the use of sol-gel and electrospinning techniques in preparation of alumina borosilicate ceramic nanofibres was demonstrated. Electrospinnability of the precursor solutions was ensured by the adjustment of viscosity of the solutions with polymeric additions. Electrospinning of these solutions into nanofibre composites was followed by the calcination of the electrospun fibres to obtain pure ceramic fibres.

2. Experimental

Materials. A target alumina borosilicate composition ($0.8\text{SiO}_2 \times 0.1\text{Al}_2\text{O}_3 \times 0.1\text{B}_2\text{O}_3$) with low boron content was selected. Alumina borosilicate fibres with this final composition were prepared by a proper heat treatment of the electrospun alumina borosilicate/PVA composite. Sol-gel solutions used in electrospinning were composed of tetraethyl orthosilicate (TEOS, $\text{Si}(\text{C}_2\text{H}_5\text{O})_4$, Sigma-Aldrich, >98%), aluminum isopropoxide ($\text{Al}(\text{OC}_3\text{H}_7)_3$, Sigma-Aldrich, >97%), triethyl borate ($\text{B}(\text{OC}_2\text{H}_5)_3$, Sigma-Aldrich, >99%), polyvinyl alcohol (PVA, Sigma-Aldrich), hydrochloric acid, absolute ethanol (EtOH), isopropyl alcohol (*i*-PrOH) and doubly deionized water.

Preparation of electrospinning solution. Success in electrospinning of mixed alkoxide solutions depends heavily on the control over the hydrolysis rates of individual alkoxides and the polymers used. Therefore the selection of the alkoxide, solvent, polymer and a suitable mixing procedure are a priority. For example, initially selected aluminum alkoxide (aluminum ethoxide) was replaced by aluminum isopropoxide owing to the fact that bigger alkoxide groups decreased hydrolysis rates. Furthermore, the mixing of PVA with the alkoxides independently was found to slow down the hydrolysis rates of alkoxides, providing the means of control on sol-gel kinetics of the final mixture. The PVA and the three alkoxide solutions were prepared as follows:

PVA solution was prepared by stirring respective amounts of PVA powder and deionized water at 80 °C for 1 h. Then, the solution was cooled down to room temperature and stirred for 24 hours. TEOS was first mixed with EtOH in a beaker, and then partially hydrolyzed for 1 h with the addition of appropriate amount of acidic solution ($\text{H}_2\text{O}/\text{HCl}$) (solution A). Into the PVA solution placed in a beaker, acidic solution, isopropyl alcohol and triethyl borate were added in the respective order (solution B). Solution C was prepared like solution B except that in the final step the aluminum isopropoxide was used instead of triethyl borate.

For the final solution, solutions B and C were simultaneously added drop-wise into solution A and a transparent viscous solution of alumina borosilicate/PVA was obtained. In this work, three different solution mixtures (see Table 1) were used. The flow of the process is summarized in Fig. 1. Upon removal of remnant solvents and PVA from the electrospun fibres, the following final molar ratio was expected: $0.8\text{SiO}_2 \times 0.1\text{Al}_2\text{O}_3 \times 0.1\text{B}_2\text{O}_3$.

Table 1. Composition of the electrospinning solutions

Solution ^a	Solution A	Solution B		Solution C	
	TEOS:EtOH:H ₂ O:HCl (molar)	BEH ^b (molar)	BEH : PVA (by weight)	APH ^c (molar)	APH : PVA (by weight)
1	1:10:2:0.01	1:10:8	1:1	1:20:8	1:1
2	1:10:2:0.01	1:10:8	1:3	1:20:8	1:3
3	1:15:2:0.01	1:15:8	1:4	1:20:8	1:4

^aSolution viscosities: 1 – 2.42 P, 2 – 6.50 P, 3 – 4.60 P.

^bBEH – B(OC₂H₅)₃:EtOH:HCl

^cAPH – Al(OC₃H₇)₃:i-PrOH:HCl

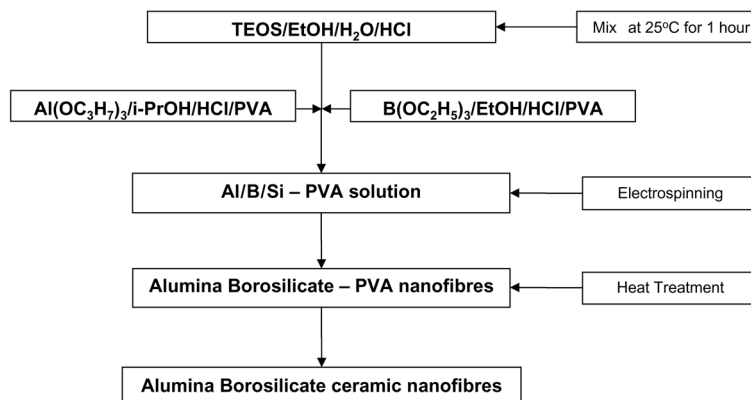


Fig. 1. Flow-chart of the alumina borosilicate ceramic nanofibre production

Preparation of nanofibres. Alumina borosilicate/PVA solutions prepared as given in Table 1 (solutions 1, 2, 3) were placed in a plastic capillary with a copper wire connected to a high voltage generator (Gamma High Voltage Research Inc., Model ES30-20W). A grounded metal drum covered with an aluminum foil, used as a collector, was placed in front of the capillary. The capillary was placed at the angle of 15° to the horizontal position to provide a uniform flow of the solution. The distance between the tip of the capillary and metal collector was varied between 7 and 15 cm. Electrospinning of the solution was performed at four voltages: 8, 10, 12 and 15 kV. Fibres pre-

pared under the applied voltages were dried initially at 70 °C for 6 h under vacuum and then calcined in air at 800, 1000 and 1200 °C for 2 h.

Characterization. For the determination of morphology and size of the nanofibres, gold sputtered samples were examined with scanning electron microscope (SEM, JSM-6400 Electron Microscope (JEOL)) equipped with NORAN System 6 X-ray Microanalysis System & Semafore Digitizer). For the determination of structure; infrared spectra of the fibres were recorded with a Bruker IFS 66/S instrument in the 400–4000 cm^{-1} range and X-ray diffraction patterns (XRD) were collected by using a Philips PW 1140 X-ray powder diffractometer with CuK_{α} radiation and a Ni filter. Combined differential thermal analysis (DTA) and thermogravimetric analysis (TG) were carried out between 25 and 1300 °C (10 °C/min) using a Rigaku (Model No. 2.22E2) system.

3. Results and discussion

3.1. Electrospinnability of sol-gel solutions

In mixing of metal alkoxides for preparation of a suitable sol-gel electrospinning solution, the addition sequence of the components and the duration of stirring have a strong influence on the electrospinnability of the solutions. TEOS is a slowly hydrolyzing alkoxide compared to aluminum isopropoxide and triethyl borate. In order to obtain a starting solution, in which all alkoxides have been evenly hydrolyzed before electrospinning, hydrolysis of TEOS was initiated one hour before the hydrolysis of aluminum isopropoxide and triethyl borate. After the preliminary experiments, it was found that the imperfections in the fibre forms (i.e., extensive bead formation and dendritic growth) could be reduced by dissolving each alkoxide in its parent alcohol. Nevertheless, in the absence of hydrochloric acid, with the 'alkoxide-parent alcohol-PVA' solutions (pH \approx 4), the beading tendency continued. Upon addition of hydrochloric acid (pH \approx 1) into the 'alkoxide-parent alcohol-PVA' solutions desired fibre morphologies were achieved (solution 1, viscosity of 2.42 P). In Figure 2, the micrographs of the fibres obtained by the electrospinning of solution 1 are shown.

The slight beading tendency that was still prominent could be overcome with a further adjustment of the viscosity of this 'primary' solution. The imperfect and slightly beaded morphology could be prevented by increasing the viscosity of the solution with further additions of PVA. Micrographs of fibres collected by the electrospinning of solution 2 are given in Fig. 3 (solution 2, 6.50 P).

Although fibre morphologies observed were found satisfactory for investigation of the other experimental parameters, the high viscosity prevented continuous flow of the electrospinning solution 2. Rather than decreasing the viscosity by decreasing the PVA concentration, increasing the ethyl alcohol concentration was found more appropriate for a 'continuous' electrospinning process. Micrographs of fibres collected by the electrospinning of solution 3 are given in Fig. 4 (solution 3, 4.60 P).

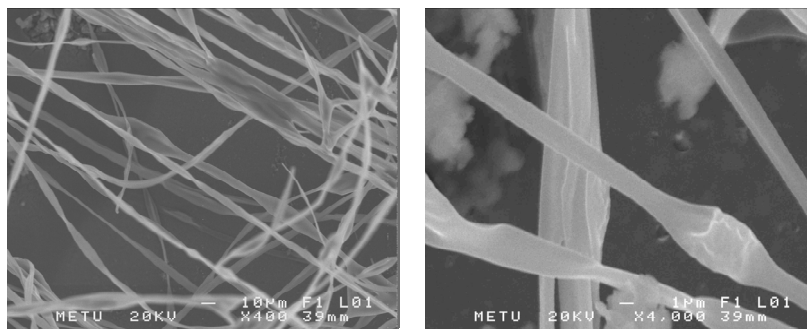


Fig. 2. Alumina borosilicate/PVA nanofibres obtained by electrospinning of solution 1 (2.42 P) (12 kV, 10 cm, pH≈1)

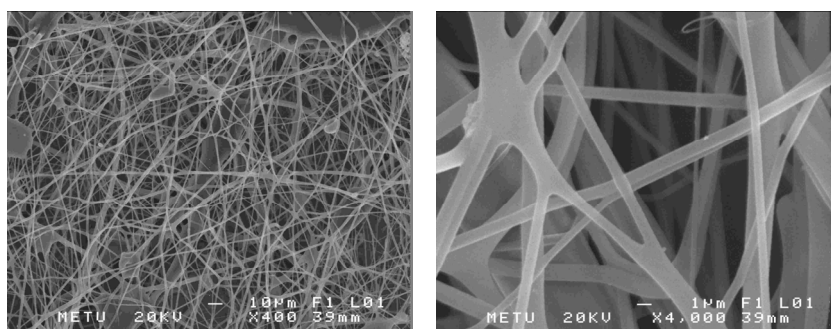


Fig. 3. Alumina borosilicate/PVA nanofibres obtained by electrospinning of solution 2 (6.50 P) (12 kV, 10 cm, pH≈1)

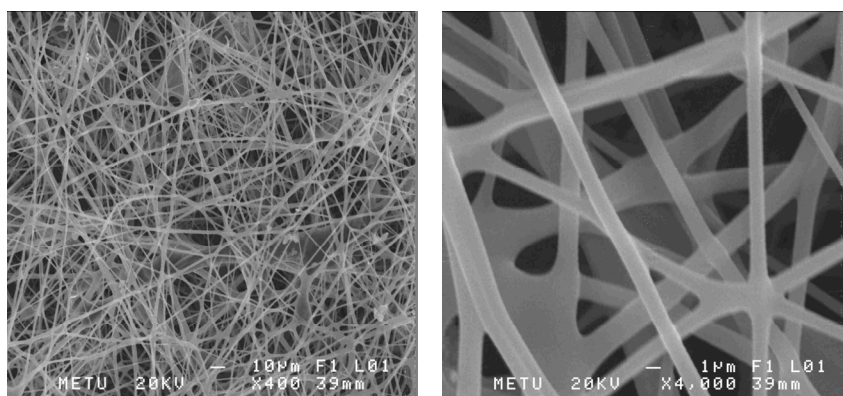


Fig. 4. Alumina borosilicate/PVA nanofibres obtained by electrospinning of solution 3 (4.60 P) (12 kV, 10 cm, pH≈1)

3.2. Parameters affecting the morphology and size of nanofibres

After the critical parameters affecting the electrospinnability of the sol-gel solutions were optimised, the experimental parameters, i.e., applied voltage and capillary

tip to metal collector distance controlling the nanofibre dimensions were studied closely. The applied voltages were 8, 10, 12 and 15 kV at a tip to collector distance of 15 cm, while the effect of distance was evaluated at 7, 10 and 15 cm with the applied voltage of 15 kV. The electrospinning results obtained at various voltages and tip to collector distances are given in Figs. 5 and 6, respectively.

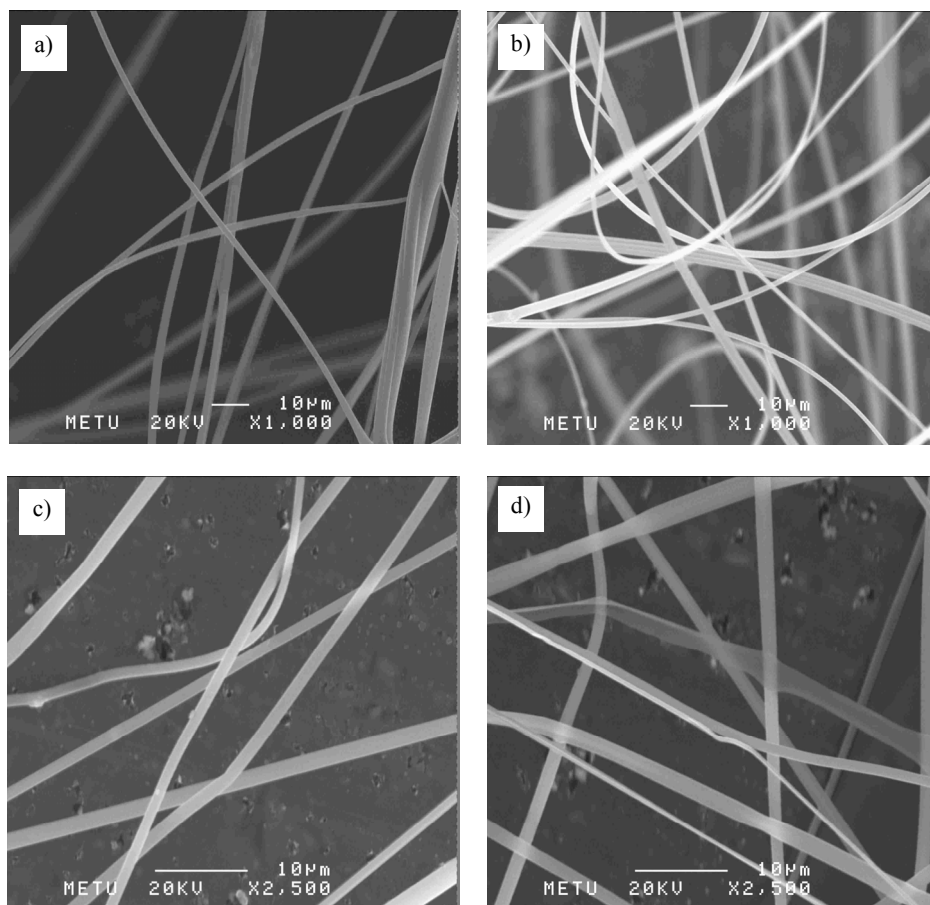


Fig. 5. Alumina borosilicate/PVA nanofibres obtained by electrospinning of solution 3 at a capillary tip to metal collector distance of 15 cm and four voltage values: a) 8, b) 10, c) 12 and d) 15 kV

Tilting the capillary by 15° with respect to the horizontal axis warranted a uniform flow and accumulation of a droplet free loose fibre mat. Micrographs taken from such fibre mats were suitable for image analysis. The changes in average fibre diameters with variations in voltage values and tip to collector distances were obtained by image analysis and are summarized in Tables 2 and 3.

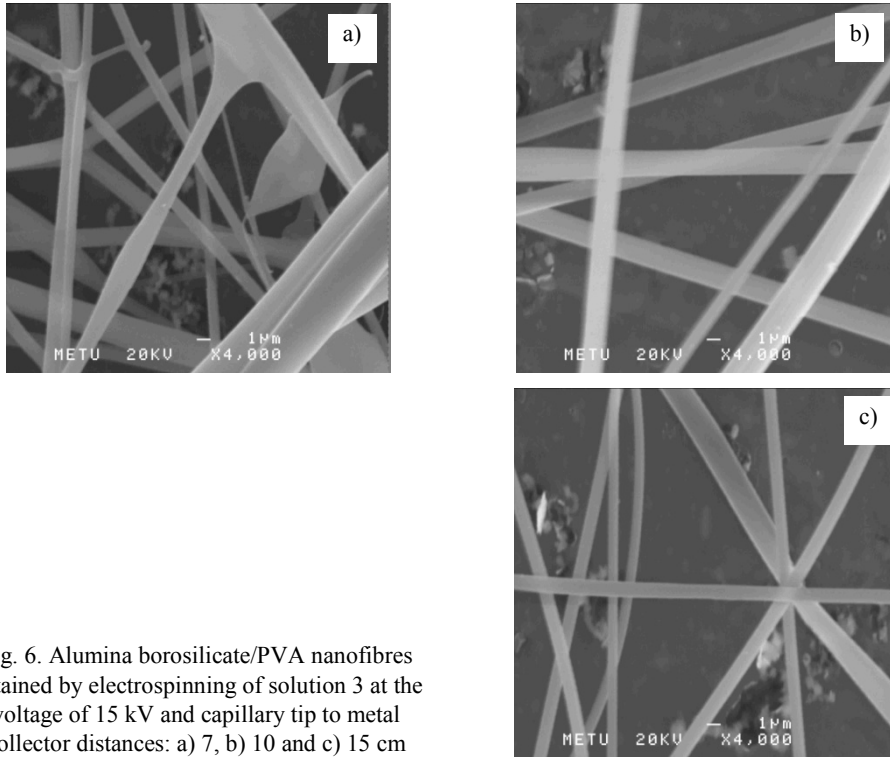


Fig. 6. Alumina borosilicate/PVA nanofibres obtained by electrospinning of solution 3 at the voltage of 15 kV and capillary tip to metal collector distances: a) 7, b) 10 and c) 15 cm

Table 2. Variation of fibre diameters with applied voltage ($l = 15$ cm)

Voltage [kV]	Average fibre diameter [nm]	Standard deviation [nm]
8	2226	407
10	2012	676
12	1290	368
15	871	183

Table 3. Variation of fibre diameters with capillary tip to metal collector distance ($V = 15$ kV)

Tip to collector distance [cm]	Average fibre diameter [nm]	Standard deviation [nm]
7	1270	631
10	1233	426
15	871	183

Measured fibre diameters decrease on increasing the applied voltage; the most pronounced effect occurs between 10 kV and 12 kV. In addition, standard deviation of measurements at higher voltage values is smaller. This implies that the fibre diameters show more uniform distribution with increasing voltage. Increasing the capillary tip to metal collector distance over 10 cm had a profound effect on the thinning of fibre di-

ameters. About a 30% decrease in the fibre diameter could be achieved at the tip to collector distance of 15 cm instead of 10 cm.

3.3. Alumina borosilicate ceramic nanofibres

The results of simultaneous TG and DTA analysis of the alumina borosilicate/PVA fibres are given in Fig. 7. In the DTA curve, there are three endothermic peaks around 130, 192 and 205 °C corresponding to the loss of absorbed water, decomposition of alkoxide alkyl groups and the pyrolysis of PVA by the dehydration on the polymer side chain, respectively [18]. The weight loss in this range was observed to be about 70%. The exothermic peaks at about 420, 440, 462 and 550 °C in the DTA curve were ascribed to the continuing decomposition of the main chain of PVA [19]. There was only about 7.3% weight loss from 400 °C up to 700 °C. No further weight loss above 700 °C indicated the formation of pure inorganic oxide in a crystalline form.

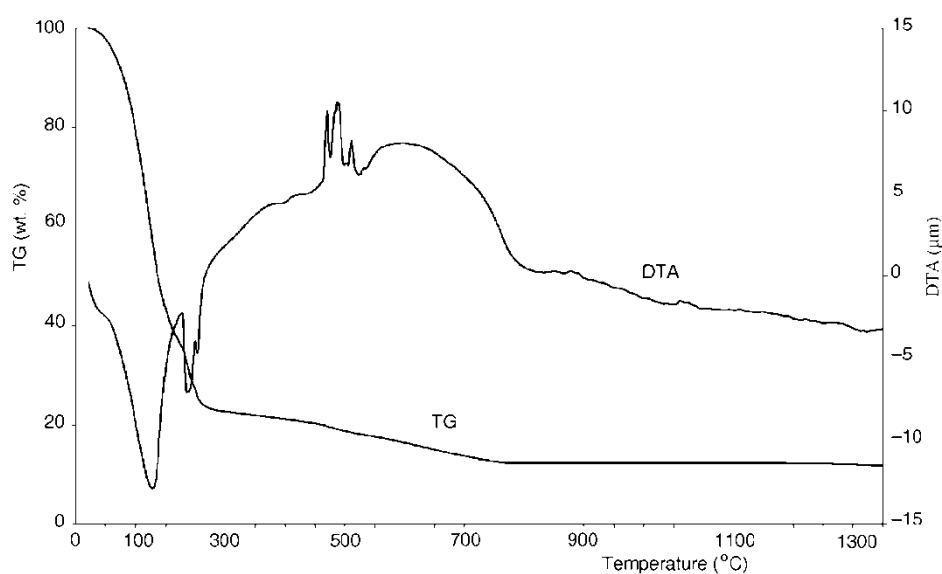


Fig. 7. TG and DTA analysis results of alumina borosilicate/PVA nanofibres obtained by electrospinning of solution 3

The dried electrospun fibre mats were heat treated at 800 °C, 1000 °C and 1200 °C for 2 h. The effect of heat treatment on the morphologies is presented in Fig. 8. At 1000 °C and 1200 °C, calcination caused sintering of the fibres through fibre interconnects and so the loss of the fibre structure due to the uncontrolled association of the fibres. On the other hand, calcination at 800 °C was promising since its effect on the fibre morphology was minimal. While the decomposition of PVA and other organics slightly deformed the fibres, the fibre diameters had shrunk about another 30% upon removal of organic content.

3.4. Structural characterization

In Figure 9, the FTIR spectra collected from as-prepared and dried alumina borosilicate/PVA nanofibres and alumina borosilicate ceramics obtained by calcination at 600, 800, 1000 and 1200 °C are given. As it can be seen in Fig. 9A, the alumina borosilicate/PVA fibres show a broad peak around 3400 cm^{-1} . The presence of such an absorption along with the absorptions at 1650 and 578 cm^{-1} implies the presence of water and hydroxyl groups that are excessively hydrogen bonded. Hydrogen bonding that hinders the in-plane OH deformations causes a shift to higher frequencies (530 to 580-700 cm^{-1}), which is another support for the above assignment. The remaining absorption peaks observed at room temperature can be attributed to the remnant solvents, PVA and the alkoxides associated with the PVA molecules [20, 21].

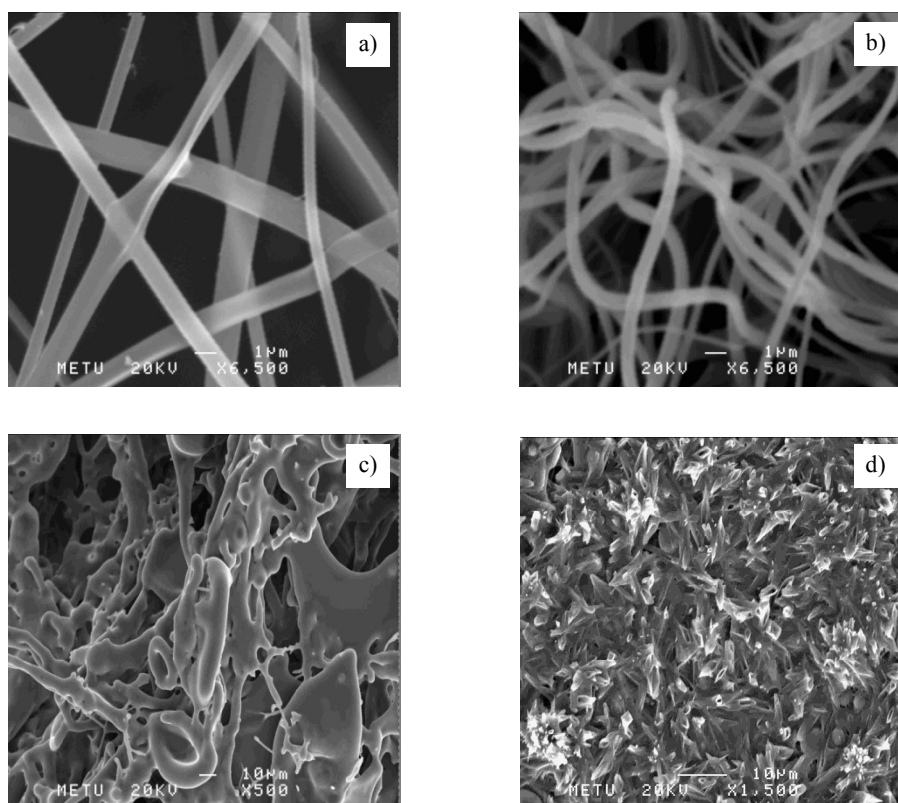


Fig. 8. The as-prepared alumina borosilicate/PVA nanofibres (a) (solution 3, 15 kV, 15 cm) and alumina borosilicate ceramics obtained by calcination of these nanofibres at: b) 800 °C, c) 1000 °C, d) 1200 °C

In accordance with the TG-DTA results, calcination at 600 °C is insufficient to burn off all the organic content. After calcination above 800 °C, the absorption bands due to hydrogen bonded hydroxyls and the organic species disappear, whereas the group of bands at 400–1600 cm^{-1} , some of which already existed in the dried sample,

becomes prominent and can be attributed to the formation of the crystalline inorganic phase. Broad absorption bands at $1400\text{--}1450\text{ cm}^{-1}$ and $1000\text{--}1200\text{ cm}^{-1}$ and relatively better defined signatures at 910 cm^{-1} , 790 cm^{-1} , 670 cm^{-1} and 455 cm^{-1} can be assigned to; B–O–Si [22], Si–O–Si and/or Al–O–Si [23], B–O–Si [24], Si–O–Si (bending) [22], B–O–Si [22], Si–O–Si and/or Al–O–Si (bending) [25] modes, respectively.

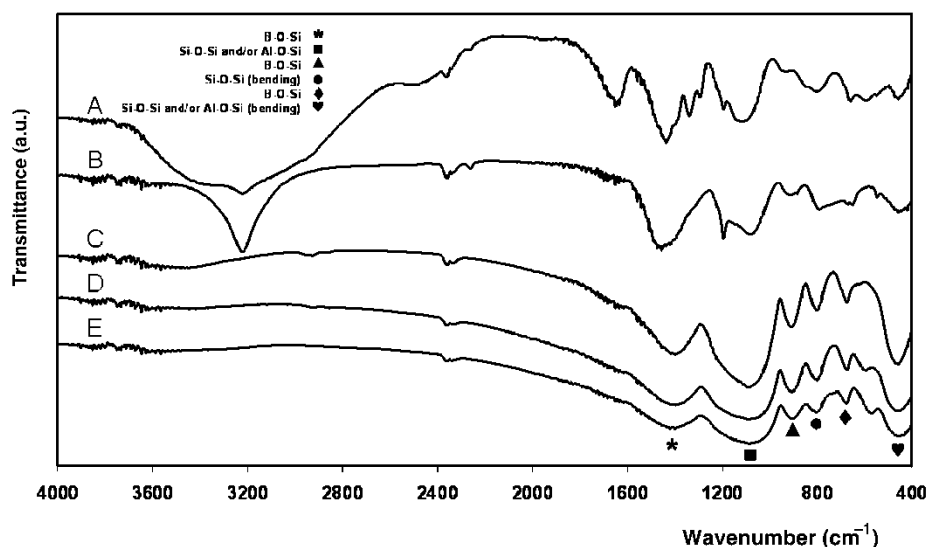


Fig. 9. FTIR spectra of as-prepared alumina borosilicate/PVA nanofibres (solution 3, 15 kV, 15 cm) (A) and alumina borosilicate ceramics obtained by calcination of the nanofibres at: B) 600 °C, C) 800 °C, D) 1000 °C, E) 1200 °C

Al–O–Si stretching mode normally corresponds to 1050 cm^{-1} [26]. The strong absorption from Si–O–Si mode possibly hinders the clear observation of such a mode due to its broad background. A similar observation is also valid for the other strong absorption at 455 cm^{-1} . Further crystallization at 1000 °C induces a new peak around 600 cm^{-1} , which may be assigned to Al–O stretching mode in AlO_6 (Fig. 9D) [27].

Like TG-DTA results, infrared data also suggests that any thermal treatment would need to be performed at temperatures higher than 600 °C to burn off all the additives. It can also be inferred from the results that the sol-gel process developed in this work is not only well-optimized for the electrospinning process, but also for bringing the three components (Si/Al/B) in close coordination.

The XRD patterns of the calcined alumina borosilicate/PVA fibres are given in Fig. 10. Crystallization initiates at temperature as low as 600 °C but, as expected, reaches appreciable levels only above 800 °C within the time frame studied (2 h of soak at set temperature). Analyses indicate that the XRD peaks emerging above 700 °C belong mainly to mullite ($\text{Al}_6\text{Si}_2\text{O}_{13}$) and to some extent $\text{Al}_4\text{B}_2\text{O}_9$ structures [28]. Also, there is a broad background around 22° which is the characteristic of vitreous SiO_2

[29]. At 1000°C, vitreous SiO₂ crystallizes. The sharp peak at 22° was assigned to a type of crystalline SiO₂, cristobalite [30]. In addition, new XRD peaks appear indicating the presence of Al₁₈B₄O₃₃ crystals [28].

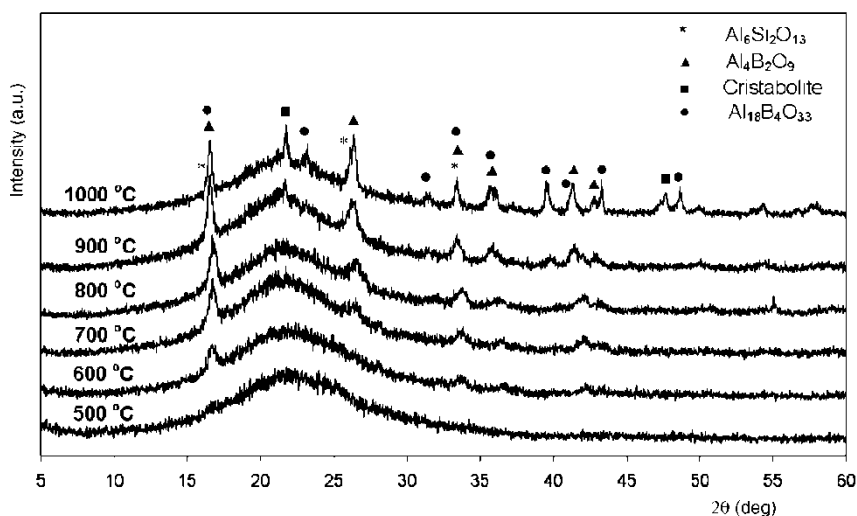


Fig. 10. XRD patterns of alumina borosilicate ceramic nanofibres calcined at various temperatures

XRD results suggest that the structure starting to form above 600 °C, is not a single phase. Although crystallization is not complete at 800 °C within 2 h, it can safely be predicted that it would be promoted by increasing the soak period at this temperature. A significantly lower crystallization temperature is typical of many mixed oxide systems synthesized via the sol-gel process, since the atomic level mixing of the components provides smaller diffusion distances that cannot be achieved with solid state reactions of the oxide components [31]. A heat treatment schedule that would be designed for slower burn-out of the organics between 400 and 500 °C besides the longer soak at 800 °C, would assure crystallization with minimal deformation on the fibre morphology.

4. Conclusions

Alumina borosilicate/PVA fibres were prepared by the sol-gel method and electrospinning technique. A sol-gel recipe that allows the formation of a homogeneous three component alkoxide solution and provides a control over solution viscosity for electrospinning process was developed. Effects of applied voltage and the capillary tip to metal collector distance on the electrospun fibre diameters were studied. Increasing the applied voltage and capillary tip to metal collector distance were found to decrease the as-spun fibre diameters. Alumina borosilicate ceramic nanofibres, with diameters down to 300 nm, were obtained via high temperature calcination. Al₆Si₂O₁₃, Al₄B₂O₉ crystals and vitreous silica were formed at 800 °C. At 1000 °C the fibre structure disap-

peared due to the uncontrolled association of the fibres. A longer soak at 800 °C is proposed for achieving the desired crystal structure while preserving the fibre morphology.

Acknowledgements

This work was supported by Turkish Scientific and Technical Research Council (TÜBİTAK) under Grant No. MAG-273.

References

- [1] MOUCHON E., COLOMBAN P., *Composites*, 26 (1995), 175.
- [2] ZHU D., JILAVI M., KRIVEN W., *Ceram. Eng. Sci. Proc.*, 18 (1997), 31.
- [3] CHEN Y., LI J., J. D., *Chem. Phys. Lett.*, 344 (2001), 450.
- [4] LIU Z., ZHOU W., SUN L., TANG D., ZOU X., LI Y., WANG Y., XIE S., *Chem. Phys. Lett.*, 341 (2001), 523.
- [5] ZHU Y., HU W., HSU W., *Adv. Mater.*, 11 (1999), 844.
- [6] READEY M., *J. Am. Cer. Soc.*, 75 (1992), 3452.
- [7] SRINIVASAN D., RAO R., ZRIBI A., *J. Electr. Mater.*, 35 (2006), 504.
- [8] SIGMUND W., YUH J., PARK H., MANEERATANA V., PYRGIOTAKIS G., DAGA A., TAYLOR J., NINO J.C., *J. Am. Cer. Soc.*, 89 (2006), 395.
- [9] MCCANN J.T., CHEN J.I.L., LI D., YE Z.-G., XIA Y., *Chem. Phys. Lett.*, 424 (2006), 162.
- [10] LI D., MCCANN J.T., XIA Y., MARQUEZ M., *J. Am. Cer. Soc.*, 89 (2006), 1861.
- [11] KIM H.-W., KIM H.-E., *J. Nanosci. Nanotechn.*, 6 (2006), 505.
- [12] AZAD A.-M., *Mater. Sci. Eng. A*, 435–436 (2006), 468.
- [13] ZHANG G., KATAPHINAN W., TEYE-MENSAH R., KATTA P., KHATRI L., EVANS E.A., CHASE G.G., RAMSIER R.D., RENEKER D.H., *Mater. Sci. Eng. B: Solid-State Mater. Adv. Techn.*, 116 (2005), 353.
- [14] WANG M., HSIEH A.J., RUTLEDGE G.C., *Polymer*, 46 (2005), 3407.
- [15] KIM G.-M., LACH R., MICHLER G.H., CHANG Y.-W., *Macromol. Rapid Comm.*, 26 (2005), 728.
- [16] SHAO C., KIM H., GONG J., LEE D., *Nanotech.*, 13 (2002), 635.
- [17] DAI H., GONG J., KIM H., LEE D., *Nanotech.*, 13 (2002), 674.
- [18] KOJI N., TOMONORI Y., KENJI I., FUMIO S., *J. Appl. Polym. Sci.* 74 (1999), 133.
- [19] CHIKAKO N., TAKEO S., TOSHIO Y., MASATAKA S., *Fuel*, 77 (1998), 321.
- [20] LIU Y., REN W., ZHANG L., YAO X., *Thin Solid Films*, 353 (1999), 124.
- [21] NAKAMOTO K., *Infrared and Raman Spectra of Inorganic and Coordination Compounds, Part B: Applications in Coordination, Organometallic, and Bioinorganic Chemistry*, Wiley, New York, 1997.
- [22] NAKAMOTO K., *Infrared and Raman Spectra of Inorganic and Coordination Compounds, Part A: Theory and Applications in Inorganic Chemistry*, Wiley, New York, 1997.
- [23] NAKANE K., YAMASHITA T., IWAKURA K., SUZUKI F., *J. Appl. Polym. Sci.*, 74 (1999), 133.
- [24] KERN W., *RCA Review*, 32 (1993), 429.
- [25] POH N., NUR H., M. M., HAMDAN H., *Catal. Today*, 114 (2006), 257.
- [26] ANDRIANOV K., BRADLEY D., *Metalorganic Polymers*, Polymer Reviews, Interscience, New York, 1965.
- [27] SOPICKA-LIZER M., *Euroceramic, Elsevier Appl. Sci.*, 1 (1989), 1609.
- [28] HAMZAWY E., ALI A., *Ceramics Int.*, 27 (2001), 607.
- [29] RAINHO J., ROCHA J., CARLOS L., ALMEIDA R., *J. Mater. Res.*, 16 (2001), 2369.
- [30] XU J., THOMPSON S., O'KEEFE E., PERRY C., *Mater. Lett.*, 58 (2004), 1696.
- [31] BRINKER C., SCHERER W., *Sol-Gel Processing*, Pergamon Press, London, 1990.

Received 14 December 2006

Revised 8 February 2007